


ORIGINAL ARTICLE

NH₂-terminal fragment of ZF21 protein suppresses tumor invasion via inhibiting the interaction of ZF21 with FAK

Makoto Nagano¹ | Daisuke Hoshino^{2,3} | Jiro Toshima¹ | Motoharu Seiki⁴ | Naohiko Koshikawa^{2,5} 

¹Department of Biological Science and Technology, Tokyo University of Science, Tokyo, Japan

²Division of Cancer Cell Research, Kanagawa Cancer Center Research Institute, Yokohama, Japan

³Organoid Biology Unit, Kanagawa Cancer Center Research Institute, Yokohama, Japan

⁴Division of Cancer Cell Research, Institute of Medical Science, University of Tokyo, Minato-ku, Japan

⁵Department of Life Science and Technology, Tokyo Institute of Technology, Yokohama, Japan

Correspondence

Makoto Nagano, Department of Biological Science and Technology, Tokyo University of Science, Nijuku 6-3-1, Katsusika-ku, Tokyo 125-8585, Japan.
Email: m.nagano@rs.tus.ac.jp

Naohiko Koshikawa, Department of Life Science and Technology, Tokyo Institute of Technology, 259 (B-19) Nagatsuda-cho, Midori-ku, Yokohama 226-8501 Japan.
Email: nkoshi-tyk@umin.ac.jp

Funding information

Takeda Science Foundation; Princess Takamatsu Cancer Research Fund; The Grant-in-Aid for Scientific Research on Innovative Areas, Grant/Award Number: JP 17H06329; KAKENHI, Grant/Award Number: JP 17K09027, JP 17K15005 and JP 23790109

Abstract

Cellular migration, coupled with the degradation of the extracellular matrix (ECM), is a key step in tumor invasion and represents a promising therapeutic target in malignant tumors. Focal adhesions (FAs) and invadopodia, which are distinct actin-based cellular structures, play key roles in cellular migration and ECM degradation, respectively. The molecular machinery coordinating the dynamics between FAs and invadopodia is not fully understood, although several lines of evidence suggest that the disassembly of FAs is an important step in triggering the formation of invadopodia. In a previous study, we identified the ZF21 protein as a regulator of both FA turnover and invadopodia-dependent ECM degradation. ZF21 interacts with multiple factors for FA turnover, including focal adhesion kinase (FAK), microtubules, m-Calpain, and Src homology region 2-containing protein tyrosine phosphatase 2 (SHP-2). In particular, the dephosphorylation of FAK by ZF21 is a key event in tumor invasion. However, the precise role of ZF21 binding to FAK remains unclear. We established a method to disrupt the interaction between ZF21 and FAK using the FAK-binding NH₂-terminal region of ZF21. Tumor cells expressing the ZF21-derived polypeptide had significantly decreased FA turnover, migration, invadopodia-dependent ECM degradation, and Matrigel invasion. Furthermore, the expression of the polypeptide inhibited an early step of experimental lung metastasis in mice. These findings indicate that the interaction of ZF21 with FAK is necessary for FA turnover as well as ECM degradation at the invadopodia. Thus, ZF21 is a potential regulator that coordinates the equilibrium between FA turnover and invadopodia activity by interacting with FAK.

KEYWORDS

extracellular matrix, focal adhesion kinase, invadopodia, tumor metastasis, ZF21 protein

Abbreviations: FA, focal adhesion; FAK, focal adhesion kinase; MT, microtubule; MT1-MMP, membrane-type I matrix metalloproteinase; SHP-2, Src homology region 2-containing protein tyrosine phosphatase 2.

Makoto Nagano and Daisuke Hoshino contributed equally to this work.

This is an open access article under the terms of the Creative Commons Attribution-NonCommercial License, which permits use, distribution and reproduction in any medium, provided the original work is properly cited and is not used for commercial purposes.

© 2020 The Authors. *Cancer Science* published by John Wiley & Sons Australia, Ltd on behalf of Japanese Cancer Association.

1 | INTRODUCTION

Invasion and metastasis are well characterized aspects of malignant tumors and lead to poor prognosis in cancer patients.¹⁻³ Cellular migration coupled with the degradation of the extracellular matrix (ECM) is crucial for invasive growth and intravasation of primary tumor cells, as well as for extravasation and formation of metastatic tumors. During tumor invasion, 2 types of actin-regulated membrane structures, FAs,⁴⁻⁶ and invadopodia,^{7,8} play key roles.

Focal adhesions include multiple molecules such as ECM receptor integrins, scaffold proteins, kinases, and phosphatases.⁹⁻¹¹ Binding of integrins to the ECM proteins induces clustering of the ECM receptors.¹² Scaffold molecules such as talin and vinculin are recruited to the cytoplasmic regions of the integrin clusters,¹³ leading to further accumulation of signal molecules such as FAK,¹⁴ and formation of the actin cytoskeleton networks at the site. The connections made between the actin cytoskeleton and the FAs generate cellular forces that help in the migration of the cell body. Formation of FAs stabilizes the cells in the adherent state, whereas continuous formation and turnover promote cellular migration.^{15,16} Another actin-regulated membrane structure, the invadopodium, shares various molecular components with FAs.¹⁷ Unlike FAs, invadopodia mediate degradation of the ECM. Many types of invasive tumor cells degrade the surrounding ECM barriers at the invadopodia and some normal cells, including macrophages and osteoclasts, form similar structures called podosomes.¹⁸ Invadopodia and podosomes belong to the same class of cellular structures, termed invadosomes.¹⁹ The ECM-degrading activity of invadosomes is carried out by ECM-degrading proteases such as membrane-type I matrix metalloproteinase (MT1-MMP).²⁰⁻²² Furthermore, FAs and invadopodia are associated with structurally distinct filamentous actins. The former connect to unbranched actin-based stress fibers, whereas the latter link to actin-related protein (Arp) 2/3 complex-dependent branched actin.¹⁷ The molecular machinery coordinating the dynamics between FAs and invadopodia is not fully understood, although evidence suggests that disassembly of FAs is an important step in triggering the formation of invadopodia.²³⁻²⁵

We previously identified a novel regulator for the turnover of FAs named ZF21.²⁶⁻³⁰ ZF21 protein interacts with multiple FA disassembly molecules including FAK, microtubules³¹ (MTs), m-Calpain,³² and Src homology region 2-containing protein tyrosine phosphatase 2 (SHP-2).³³ ZF21 has an FYVE domain³⁴ (41-105 amino acids [aa]) and a pleckstrin homology (PH)-like domain (106-234 aa). The FYVE domain of ZF21 is necessary to localize at the endosomal compartments and FAs through its interaction with the membrane lipid phosphatidylinositol-3-phosphate (PI3P).³⁰ The NH₂-terminal region (1-105 aa) or the COOH-terminal PH-like domain is sufficient to interact with FAK or MTs, respectively.²⁸⁻³⁰ Conversely, both regions are indispensable for binding to m-Calpain and SHP-2. ZF21 induces FA disassembly by promoting dephosphorylation of FAK in an MT-dependent manner that is required for cell migration in vitro and for tumor metastasis in mice.^{29,30} Interestingly, ZF21-depleted cells show a decrease in ECM-degrading activity at the invadopodia

without affecting the expression levels of MT1-MMP, MMP-2, and MMP-9.²⁶ ZF21 knockdown inhibits the accumulation of MT1-MMP at the invadopodium structure.²⁶ These findings suggest that ZF21 has a dual role in tumor invasion as a promoter of FA turnover and as an ECM-degrading regulator, although the precise mechanism has not been fully elucidated.

In this study, we sought to improve our understanding of the molecular mechanisms of ZF21-promoted tumor invasion, focusing on its interaction with FAK.

2 | MATERIAL AND METHODS

2.1 | Antibodies, plasmids, and reagents

We used commercially available antibodies to detect actin (C4, Millipore) and Tyr397-phosphorylated FAK (BioSource). Rhodamine-phalloidin was purchased from Thermo Fisher Scientific. All other chemical reagents were purchased from Sigma or Wako, unless otherwise indicated. We obtained the complementary DNA encoding ZF21 protein from HT1080 cells by RT-PCR. The mammalian expression vector pLenti6/V5-DEST or the *Escherichia coli* expression vectors, pDEST15 and pDEST17 (Thermo Fisher Scientific) were used to express the recombinant proteins, as described previously.³⁰

2.2 | Knockdown experiments using siRNA

The target sequences for siRNA were designed and synthesized (Thermo Fisher Scientific). The siRNA sequences were as follows: siFAK#1; 5'-GGGCCAGTATTATCAGGCATGGAGA-3', siFAK#2; 5'-CGGACAGCGTGAGAGAGAGAAATTTCT-3'. Cells were seeded (2.5×10^4 /well into 24-well plates) and transfected with a 10 nM siRNA mixture using Lipofectamine™ RNAiMAX (Thermo Fisher Scientific), in accordance with the manufacturer's instructions.

2.3 | Cell culture

HT1080 and MDA-MB231 cells were obtained from JCRB. Cells were cultured in Dulbecco's modified Eagle's medium (DMEM) supplemented with 10% fetal bovine serum (FBS), penicillin, and streptomycin and incubated at 37°C with 5% CO₂.

2.4 | In vitro protein binding assay

GST-tagged or 6× His-tagged recombinant proteins were expressed in *E. coli* BL21(DE3)pLysS using the pDEST15 or pDEST17 expression vector (Life Science Tech.), followed by purification using glutathione Sepharose 4B (GE Healthcare Life Sciences) or Ni-NTA agarose (Qiagen), respectively. HT1080 or MDA-MB231 cells cultured on a plastic plate were washed with ice-cold PBS and scraped

off in RIPA buffer (50 mM Tris-HCl, pH 7.5, 100 mM NaCl, 2 mM $MgCl_2$, 0.1% SDS, 0.5% sodium deoxycholate, 1% Triton X-100, 10% glycerol, 1 mM Na_3VO_4 , and protease inhibitor mixture set III) on ice. Lysates were centrifuged for 5 min at 20 000 g at 4°C. A fraction of the cleared lysates was incubated with 10 μ g of GST-enhanced green fluorescent protein (EGFP) and GST-ZF21, or the mutant thereof, bound to glutathione-conjugated Sepharose beads at 4°C for 6 h. Pellets containing the beads were collected, washed 3 times with ice-cold RIPA buffer, and subjected to SDS-PAGE followed by western blotting, using the indicated antibodies.

2.5 | Total internal reflection fluorescence microscopy

Live cells were observed using a UAPON 100xOTIRF/NA 1.49 (Olympus) objective on an Olympus IX83 microscope equipped with a total internal reflection fluorescence (TIRF) illuminator and fiber optic-coupled laser illumination (Olympus), and an Orca-R2-cooled charge coupled device (CCD) camera (Hamamatsu).

2.6 | FAK dephosphorylation assay

The FAK dephosphorylation assay was performed as described previously.³⁰ Briefly, cells were grown on fibronectin-coated plastic dishes and treated with 5 μ M nocodazole for 30 min to depolymerize MTs. Cells were then incubated to resume the polymerization of MTs. Cells were resolved with Laemmli sample buffer and analyzed by western blot.

2.7 | Cell migration and invasion assays

Transwell migration assays were performed as described previously.³⁰ Briefly, Transwell inserts with 8- μ m pore size filters (Corning) pre-coated on both sides with fibronectin were inserted into 24-well plates. DMEM containing 10% FBS was added to the lower chamber and a cell suspension (5×10^4 cells) was placed in the upper chamber. The plates were incubated at 37°C with 5% CO_2 for 6 h. After incubation, the cells that had migrated to the lower side were stained with 0.5% crystal violet solution or Giemsa solution and counted using a light microscope at $\times 200$ magnification. Values represent averages from 5 fields.

2.8 | Fluorescent gelatin degradation assay

The fluorescent gelatin degradation assay was performed as described previously.³⁵ Oregon Green (OG)-labeled gelatin was obtained from Invitrogen. The 35 mm glass-bottom dishes (IWAKI) were coated with 50 μ g/mL poly-L-lysine for 20 min at 25°C, washed with PBS, and fixed with 0.5% glutaraldehyde for 15 min. After 3 washes,

0.2% fluorescently labeled gelatin in PBS was incubated for 10 min at room temperature. After washing with PBS, coverslips were incubated in 5 mg/mL sodium borohydride for 5 min and washed 3 times in PBS. To assess the ability of cells to form invadopodia and degrade the gelatin, cells were plated onto OG-coated dishes in complete medium and incubated at 37°C for 6 h for HT1080 cells and 20 h for MDA-MB231 cells.

2.9 | Lung colonization assay

The lung colonization assay was examined using 6-wk-old female BALB/c nude mice (Clea). The cells were fluorescently labeled with CellTracker Green and CellTracker Orange (Thermo Fisher Scientific). Control cells and ZF21NT cells (1×10^5 each) were injected into the tail veins of nude mice, which were sacrificed 1 or 24 h later. Following lung dissection, fluorescently labeled cells were counted by confocal microscopy (Zeiss LSM 710). All mice were maintained under specific pathogen-free conditions and the experiments were performed in accordance with the institutional animal care and use committee (Kanagawa Cancer Center).

2.10 | Cell proliferation assay

Cell proliferation was measured using the Cell Counting Kit-8 (CK04, Dojindo), following the manufacturer's instructions. Cells were cultured in 96-well tissue culture plates for 48 h. After incubating the cells with the Cell Counting Kit-8 solution for 1 h, the absorbances were measured at 450 nm using the iMark microplate reader (Bio-Rad).

2.11 | Statistics

Statistical analysis was performed using GraphPad Prism 6 for Macintosh. Data are presented as the mean \pm SD or the mean \pm SEM. Statistical significance was determined using unpaired t test with Welch correction or 2-way ANOVA with post hoc Tukey test.

3 | RESULTS

3.1 | ZF21NT inhibits the interaction of ZF21 with FAK

ZF21 has 2 unique domains: a PI3P-binding FYVE domain at the 41-105 aa region (ZF21FYVE), and a novel protein folding pleckstrin homology (PH)-like domain at the 106-234 aa (ZF21PH) region.²⁹ The N-terminal 1-105 aa fragment of ZF21 (ZF21NT) is sufficient to bind to FAK but not to other identified binding partners, while the fragment lacks the promoting activities for tumor invasion and metastasis.²⁸⁻³⁰ Therefore, we expected the ZF21NT fragment to inhibit the

interaction between ZF21 and FAK in tumor cells, thereby inhibiting cell migration and tumor invasion (Figure 1A). To examine whether ZF21NT inhibits the interaction of full-length ZF21 with FAK, we utilized a GST-pull-down assay using a purified glutathione-S-transferase (GST)-tagged ZF21 protein (GST-ZF21, Figure 1B) to pull down FAK from the cell lysate in the presence of a purified hexa-histidine (6x His)-tagged ZF21NT fragment (6x His-ZF21NT; Figure 1B). GST-EGFP or 6x His-EGFP were utilized as negative controls (Figure 1B).

In accordance with our previous study, FAK bound to GST-ZF21 but not to GST-EGFP (Figure 1C, lanes 2 and 3), indicating that the assay detected the specific interaction of FAK with ZF21. Addition of the 6x His-ZF21NT fragment decreased the interaction of FAK with GST-ZF21 in a dose-dependent manner (Figure 1C, lanes 4–7), whereas 6x His-EGFP had no effect on the interaction (Figure 1C, lane 8). Thus, the ZF21NT fragment had an inhibitory effect on the interaction between ZF21 protein and FAK.

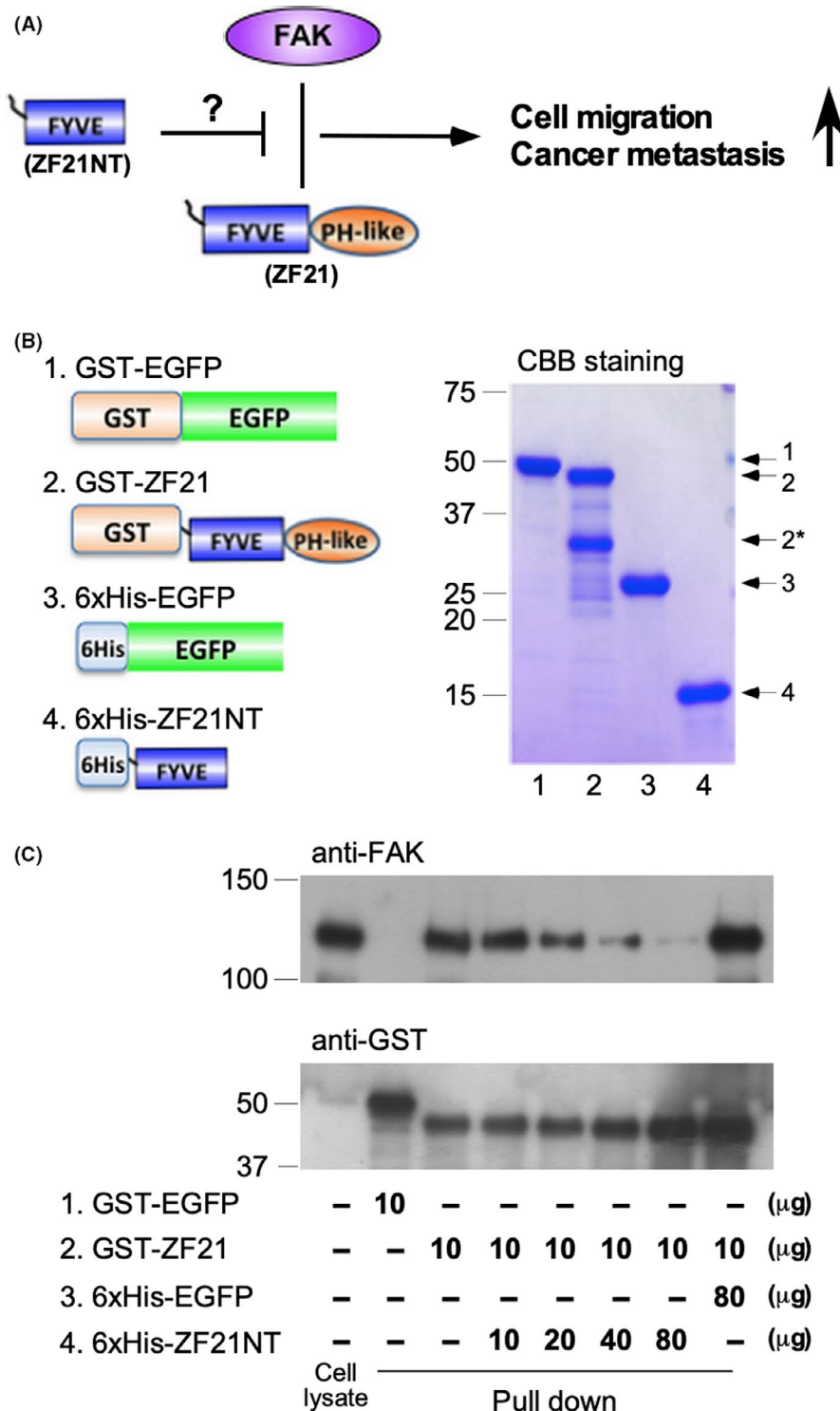


FIGURE 1 Inhibitory effect of ZF21NT fragment on ZF21 binding to FAK. A, Model proposed for ZF21NT-mediated tumor suppression, in which ZF21NT inhibits the interaction between FAK and ZF21. B, Purification of ZF21 or EGFP derivatives used for the pull-down assays. (Left) Schematic representation of ZF21 or EGFP derivatives used for the pull-down assays in (C). GST, glutathione-S-transferase tag; 6x His, hexa-histidine tag; ZF21NT, N-terminal 1-105 aa residues of ZF21 protein. (Right) Coomassie Brilliant Blue (CBB) staining of the purified recombinant proteins. Arrows indicate intact molecules of ZF21 or EGFP derivatives. Asterisk indicates the degraded form. 1, GST-EGFP; 2, GST-ZF21; 3, 6x His-EGFP; 4, 6x His-ZF21NT. C, Effect of ZF21NT on the interaction of FAK with ZF21

3.2 | ZF21NT reduces the interaction of the ZF21 protein with FAK in situ

Next, we examined if ZF21NT inhibits the interaction between ZF21 and FAK in live cells. The m1Venus-tagged form of ZF21NT was expressed in HT1080 cells (Figure 2A). Although m1Venus-ZF21NT was predominantly localized to the cytoplasm and nucleus, a fraction of ZF21NT was colocalized with mCherry-tagged FAK at the punctate-like structures (Figure 2B), indicating that ZF21NT accumulated in FAK-positive FAs. We then examined the effect of ZF21NT expression on the localization of ZF21 to FAs. ZF21NT was expressed as the V5 epitope-tagged form in HT1080 cells expressing ZF21-m1Venus (Figure 2C). We utilized TIRF microscopy to visualize ZF21 only localized at the sites of adhesion of the cells to the ECM. ZF21-m1Venus localized to FAs tagged with mCherry-FAK were observed in the control cells (Figure 2D, mock). However, the expression of V5-ZF21NT decreased the accumulation of ZF21 at FAs (Figure 2D, V5-ZF21NT). Thus, ZF21NT accumulated at FAs, resulting in the disruption of the in situ interaction of ZF21 with FAK.

3.3 | ZF21NT reduces the microtubule-dependent turnover of FAK

We next investigated if ZF21NT inhibits the turnover of phosphorylated FAK, which is promoted by ZF21 in tumor cells. In previous studies, extension of MTs to FAs promoted the dephosphorylation of FAK at pTyr397 (pY³⁹⁷-FAK) and the disassembly of the FA complex. ZF21 is required for the MT-dependent dephosphorylation of FAK.³⁰ Therefore, we evaluated the effect of ZF21NT expression on the MT-dependent turnover of phosphorylated FAK in human fibrosarcoma HT1080 cells. We utilized nocodazole (NZ), an MT inhibitor, to synchronize the cells at the FA formation state. In control cells, washout of NZ from the cells rapidly decreased the levels of pY³⁹⁷-FAK during the synchronized disassembly of FAs (Figure 3A, mock). In contrast, ZF21NT cells retained the levels of pY³⁹⁷-FAK equivalent to the original levels even after 30 min (Figure 3A, ZF21NT), suggesting that ZF21NT inhibits MT-dependent FAK dephosphorylation.

Because ZF21 interacts with SHP-2 tyrosine phosphatase,³⁰ which promotes FAK dephosphorylation in a phosphatase-dependent manner, we examined whether ZF21NT expression inhibited the dephosphorylation of FAK only in the presence of active SHP-2.

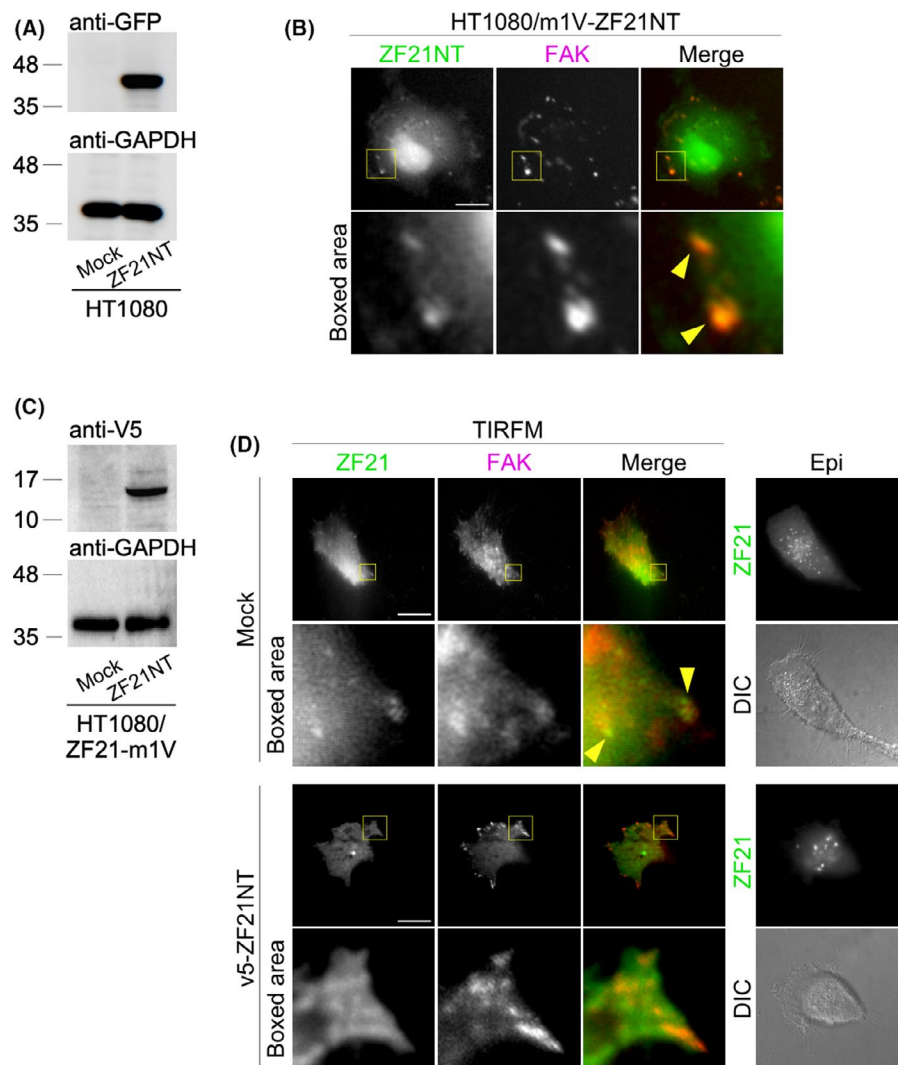


FIGURE 2 Effect of ZF21NT fragment on the ZF21 localization at FAs. A, Expression levels of m1Venus-tagged ZF21NT fragments in the cells. B, Colocalization of m1V-ZF21NT with mCherry-tagged FAK in the cells. Boxed areas are shown at a higher magnification below. Yellow arrowheads indicate the colocalization of ZF21NT and FAK. C, Expression levels of the V5-tagged ZF21NT fragment in the ZF21-m1Venus (ZF21-m1V)-expressing cells. D, After 48 h, the localization of ZF21-m1V and mCherry-FAK at the cell-ECM adhesion sites was specifically visualized by total internal reflection fluorescence microscopy (TIRFM). Intracellular distribution of ZF21-m1V was visualized under the epifluorescence microscope (Epi). Boxed areas are shown at a higher magnification below. Yellow arrowheads indicate the colocalization of ZF21 and FAK. Scale bar, 10 μ m

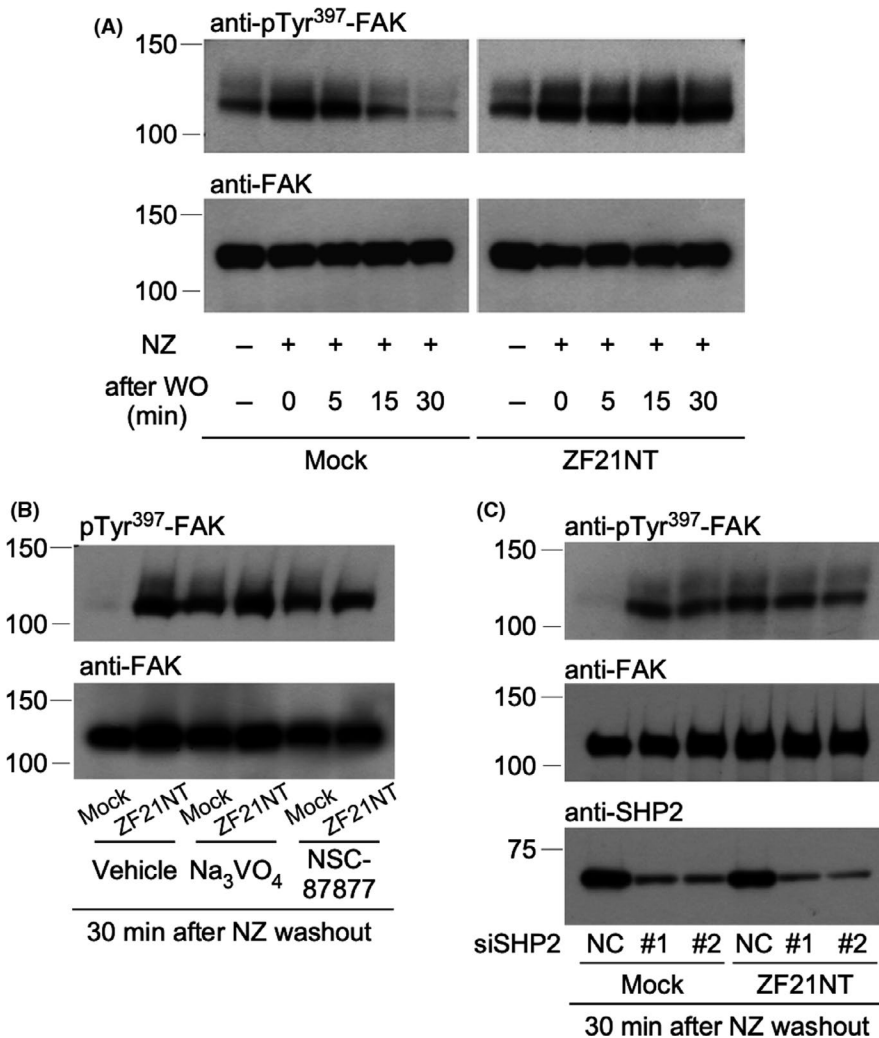


FIGURE 3 Effect of ZF21NT fragment on the microtubule-dependent FAK dephosphorylation. A, Dephosphorylation assay of FAK phosphorylated at Tyr³⁹⁷. B, Phosphatase dependency of FAK dephosphorylation at Tyr³⁹⁷ in ZF21NT expressing cells. C, SHP-2 dependency of FAK dephosphorylation at Tyr³⁹⁷ in ZF21NT expressing cells

We utilized a pan-phosphatase inhibitor, Na₃VO₄, and an SHP-2 specific inhibitor, NSC-87877.³⁶ In the presence of either of these inhibitors, the expression of ZF21NT had negligible effects on the levels of pY³⁹⁷-FAK after NZ washout (Figure 3B). SHP-2 knockdown using siRNA also diminished the effect of ZF21NT on the MT-dependent dephosphorylation of FAK (Figure 3C). The phenotypes observed in ZF21NT-expressing cells were similar to those seen in ZF21-knockdown cells. Thus, ZF21NT expression inhibits MT-dependent FAK dephosphorylation, reducing the turnover rate of active FAK.

3.4 | ZF21NT reduces FAK-dependent cell migration

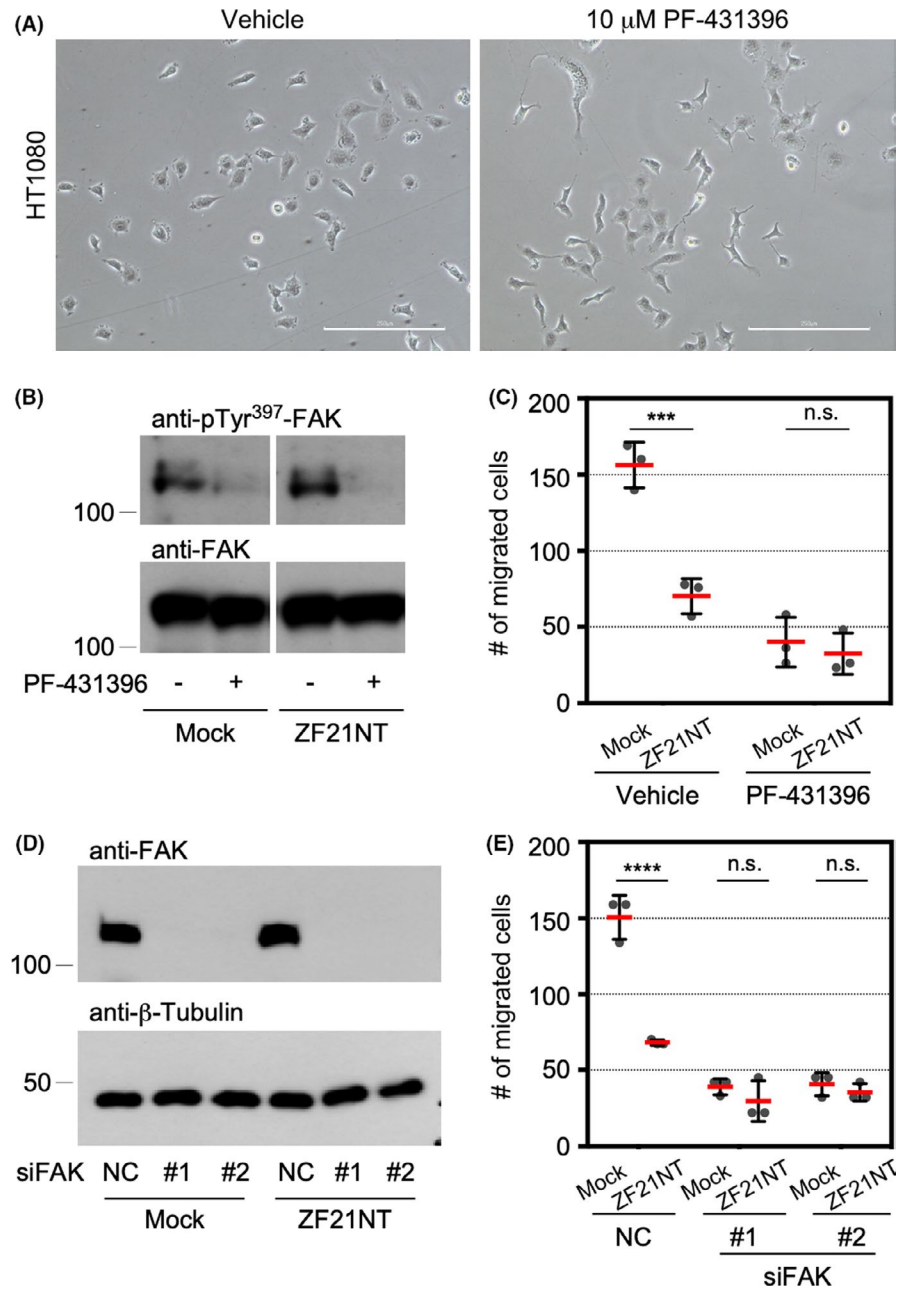
We next investigated if the expression of ZF21NT inhibits cell migration regulated by FAK. We utilized an FAK inhibitor, PF-431396, which reduces pY³⁹⁷-FAK levels.³⁷ The inhibitor had a negligible effect on cellular viability after 6 h at 10 μM (Figure 4A). However, 30 min after treatment with the inhibitor, the FAK phosphorylation levels at Tyr³⁹⁷ decreased rapidly, regardless of ZF21NT expression (Figure 4B). In the absence of the inhibitor, the migratory activity of ZF21NT-expressing cells decreased significantly, to 44.8% of that in the control mock cells, indicating that ZF21NT inhibited migratory

activity (Figure 4C, Vehicle). Conversely, in the presence of the inhibitor, ZF21NT-expressing cells exhibited similar levels of decreased migratory activity as control cells (Figure 4C, PF-431396). These results suggested that ZF21NT specifically inhibits FAK-dependent migratory activity. To confirm this, we further examined the effect of ZF21NT expression on the migratory activity of FAK-depleted cells using small-interfering RNAi (siRNA). The siRNA sequences targeting FAK mRNA (siFAK#1 and #2) individually decreased the expression levels of FAK protein (Figure 4D). As expected, FAK knockdown diminished the effect of ZF21NT expression on the migratory activity of the cells (Figure 4E). Therefore, ZF21NT inhibits FAK-dependent cell migration.

3.5 | ZF21NT inhibits invasive activity of the cells

ZF21 has been reported to regulate ECM degradation of invasive cells at the invadopodia.²⁶ Invadopodia are assembled by the formation of filamentous actin on the ECM, which are visualized as actin-rich spots. Recruitment of MT1-MMP to the actin-rich spots is indispensable for the cells to degrade the ECM at the invadopodia. Although the depletion of ZF21 decreases both ECM degradation and the

FIGURE 4 Effect of ZF21NT fragment on the migratory activity of the cells. A, Effect of the FAK inhibitor, PF-431396, on the viability of HT1080 cells. B, Phosphorylation levels of FAK at Tyr³⁹⁷ in the presence of PF-431396. C, Effect of FAK inhibitor on the migratory activity of ZF21NT expressing cells. D, Expression levels of FAK in siFAK-treated cells. E, Effect of FAK knockdown on the migratory activity of ZF21NT expressing cells. Data show mean \pm SEM from 3 independent experiments. *** $P < .005$, **** $P < .0001$, 2-way ANOVA with Tukey post hoc test. Scale bars, 250 μ m



recruitment of MT1-MMP to the actin-rich spots, the mechanism of how ZF21 regulates invadopodia-dependent ECM degradation is still unclear. Therefore, we aimed to clarify the role of ZF21-FAK interaction in ECM degradation using the ZF21NT fragment.

HT1080 cells expressing the V5 epitope-tagged ZF21NT fragment were seeded and cultured on a slide glass coated with fluorescent OG-gelatin. Invadopodia were visualized by staining actin with rhodamine-labeled phalloidin as punctate actin signals. The actin-rich spots of invadopodia were observed at the central region of the cells both in control and ZF21NT cells (Figure 5A, Actin). However, ECM degradation spots, visualized by the loss of fluorescence intensity of OG-gelatin, significantly decreased in ZF21NT-expressing cells to 31.1% compared with the control cells (Figure 5A, OG-green; Figure 5B). The effect of ZF21NT expression on HT1080 cells was similarly observed in mammary tumor-derived

MDA-MB231 cells (Figure 5C,D). These results indicated that ZF21NT inhibited invadopodia formation and thereby reduced ECM degradation. In accordance with the inhibitory effect of ZF21NT on invadopodia assembly, the invasive activity of ZF21NT-expressing cells was significantly reduced compared with that of control cells (Figure 5E,F). Thus, the interaction of ZF21 with FAK, which is inhibited by ZF21NT, appears to play crucial roles in invadopodia assembly and invasive activity of the cells.

3.6 | ZF21NT inhibits an early step of experimental lung metastasis in mice

Invasive phenotypes including upregulated migratory activity and invadopodia formation are features of highly metastatic tumor cells.

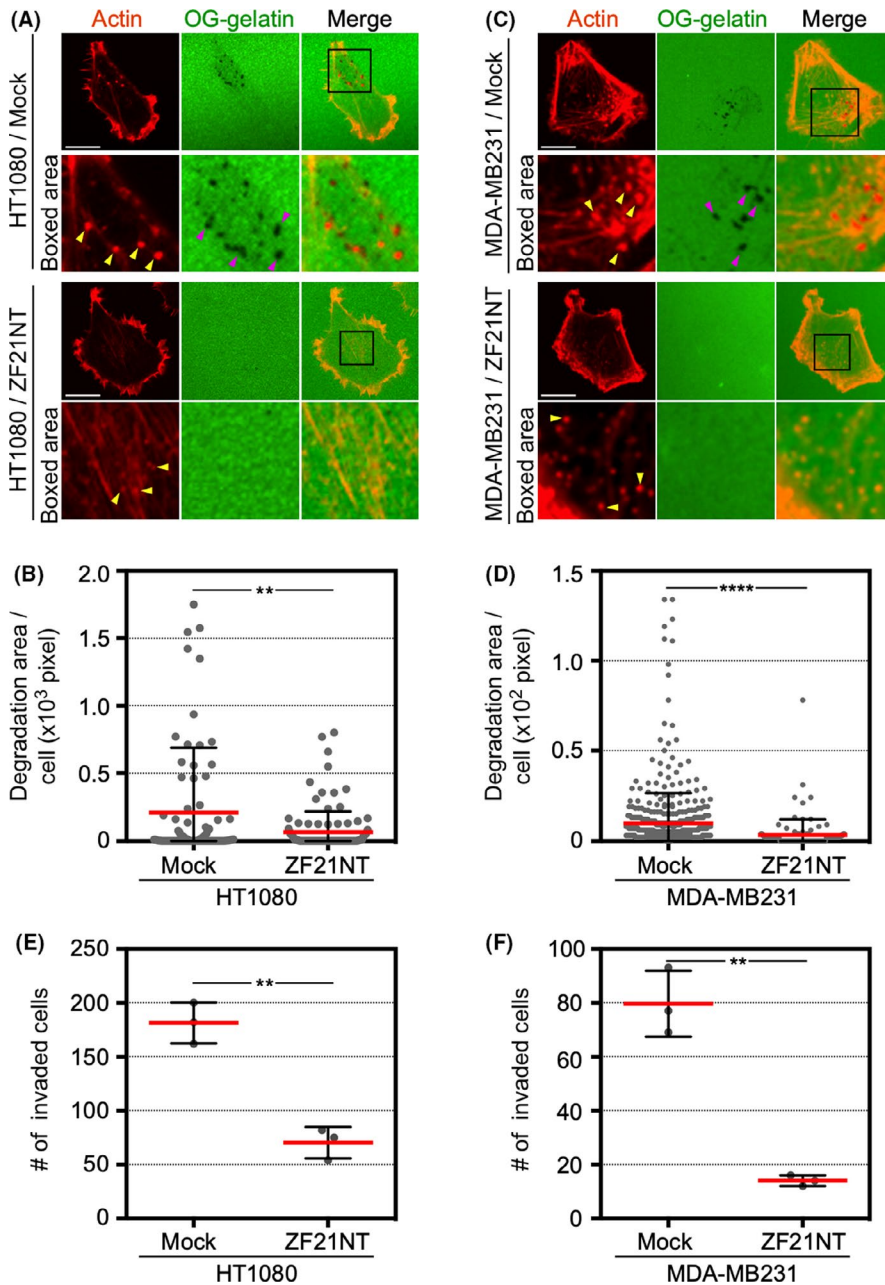


FIGURE 5 Effect of ZF21NT fragment on the ECM-degrading activity at the invadopodia. A, C, ECM-degrading activity of V5 epitope-tagged ZF21NT expressing cells, HT1080 (A), or MDA-MB231 (C), stained with phalloidin for localization of filamentous actin (actin panels). Degraded ECM appears as dark areas (OG-gelatin panels). The boxed areas are shown at higher magnification in the lower panels (boxed area). Yellow or magenta arrowheads indicate the actin-rich structures or ECM-degraded spots, respectively. B, D, Quantification of ECM degradation area at the invadopodia structures. Average degradation area per cell in (A) or (C) was calculated and presented in (B) or (D), respectively. E, F, Invasive activity of ZF21NT expressing cells, HT1080 (E) or MDA-MB231 (F). Data show mean \pm SD with at least 100 actin-rich spots (B, D) or mean \pm SEM from 3 independent experiments (E, F). ** $P < .01$, **** $P < .0001$, unpaired t test with Welch correction. Scale bar, 10 μ m

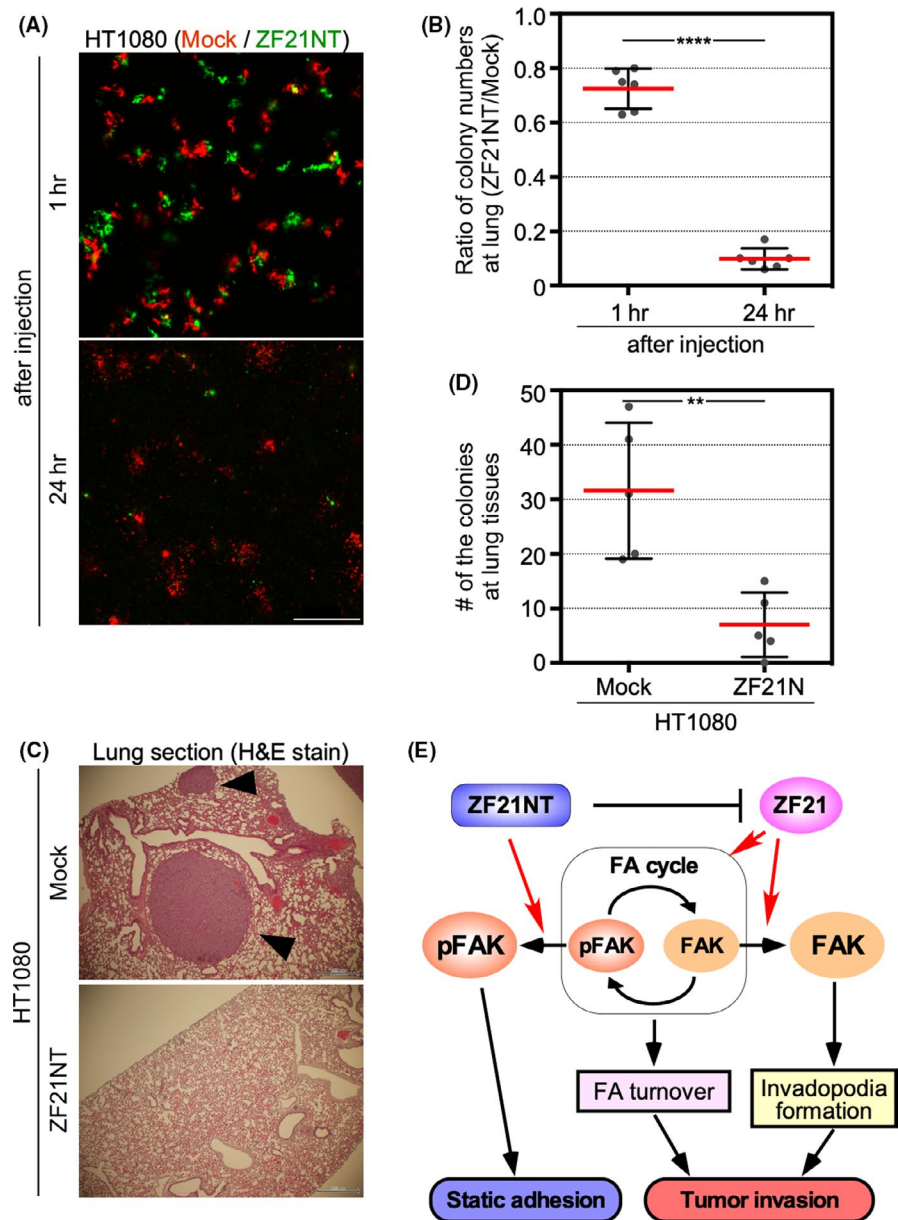
ZF21 increases the invasive activity of the cell, which is important for the metastatic spreading of tumor cells and the formation of secondary colonies.²⁹ ZF21 was confirmed to promote a step in metastasis that involves extravasation and survival of the cells in the lung tissue. Therefore, we evaluated whether ZF21NT shows an inhibitory effect, similar to ZF21 depletion, on early metastasis in an experimental metastasis assay. Similar levels of fluorescent signals of control (red) and ZF21NT (green) cells were detected in the lung tissue 1 h after injection (Figures 6A,B; 1 h). However, the fluorescent signals of ZF21NT cells were significantly lower than those of the control cells 24 h after injection (Figures 6A,B; 24 h). Because most circulating cells were cleared from the lung during the following 24 h, only the cells that escaped from the bloodstream after extravasation were detected in the lung tissue at this time point. Thus, ZF21NT-expressing cells decreased the metastatic ability of HT1080 cells at

an early step of lung metastasis. Indeed, ZF21NT-expressing cells failed to form metastatic colonies in the lung. ZF21NT-expressing cells significantly reduced the number of metastatic foci in the lung tissue 28 d after being injected into the tail vein of mice (Figures 6C,D). These results indicate that the interaction of ZF21 with FAK, which is inhibited by ZF21NT, is crucial for tumor progression.

3.7 | ZF21(41-75 aa)-derived polypeptide has an inhibitory effect on tumor invasion

Finally, we shortened the ZF21-derived peptide with an inhibitory effect on tumor invasion. To shorten the region of ZF21NT that was bound to FAK, we performed a pull-down assay using a purified GST-tagged ZF21NT-derived fragment to pull down FAK from the cell

FIGURE 6 Effect of ZF21NT fragment on lung metastasis in mice model. A, Lung metastatic colonization assay in mouse xenograft model. B, Ratio of lung metastatic colonies formed by ZF21NT cells to mock. The number of green or red fluorescent colonies in (A) was counted. C, H&E staining of murine lungs 28 d after injection of control or ZF21NT cells into the tail veins of 8-wk-old nude mice. D, The numbers of tumor nodules in (C). E, Role of ZF21 and effect of ZF21NT in tumor invasion. Data show mean \pm SEM with 6 (B) or 5 (D) lung tissues. ** $P < .01$, **** $P < .0001$, unpaired t test with Welch correction. Scale bar, 200 μ m



lysate. Firstly, we constructed 4 fragments with different lengths: 1-41 aa, 41-105 aa, 1-75 aa, and 76-105 aa regions (Figure 7A). In the assay, FAK bound to the 41-105 aa or 1-75 aa fragments, but not to the 1-41 aa or 76-105 aa fragments, based on western blot analysis of FAK pulled down with the GST-tagged fragment (Figure 7B). We then constructed shorter fragments: 41-75 aa, 41-70 aa, and 61-75 aa regions (Figure 7C). Among them, FAK bound only to the 41-75 aa fragment (Figure 7D). To elucidate the inhibitory activity of the 41-75 aa fragment peptide, ZF21(41-75), we expressed the polypeptide as the m1Venus-tagged form in HT1080 cells (Figure 7E). The invasion activity of ZF21(41-75)-expressing cells was significantly reduced compared to that of the control cells (Figure 7F). However, the inhibitory activity of the ZF21(41-75) polypeptide (37.2% inhibition, Figure 7F) was lower than that of the ZF21NT polypeptide (61.3% inhibition, Figure 3E). The ZF21(41-75) peptide did not have any effect on cellular proliferation (Figure 7G), indicating that the

peptide suppressed the invasive activity of the cells without affecting cellular viability.

4 | DISCUSSION

In this study, we demonstrated that the FAK-binding ZF21NT polypeptide has an inhibitory effect on ZF21-FAK interaction. The expression of ZF21NT in HT1080 cells inhibited FAK dephosphorylation and cell migration as effectively as the knockdown of ZF21.³⁰ Perturbation of SHP-2 function diminished the effect of ZF21NT expression on cellular activities, which was similar to diminishing the effect of ZF21 knockdown.³⁰ Furthermore, ZF21NT expression markedly reduced the ECM-degrading activity of the cells, as effectively as ZF21 knockdown.²⁶ Therefore, ZF21NT expression has an effect similar to that of ZF21 knockdown on the dynamics and

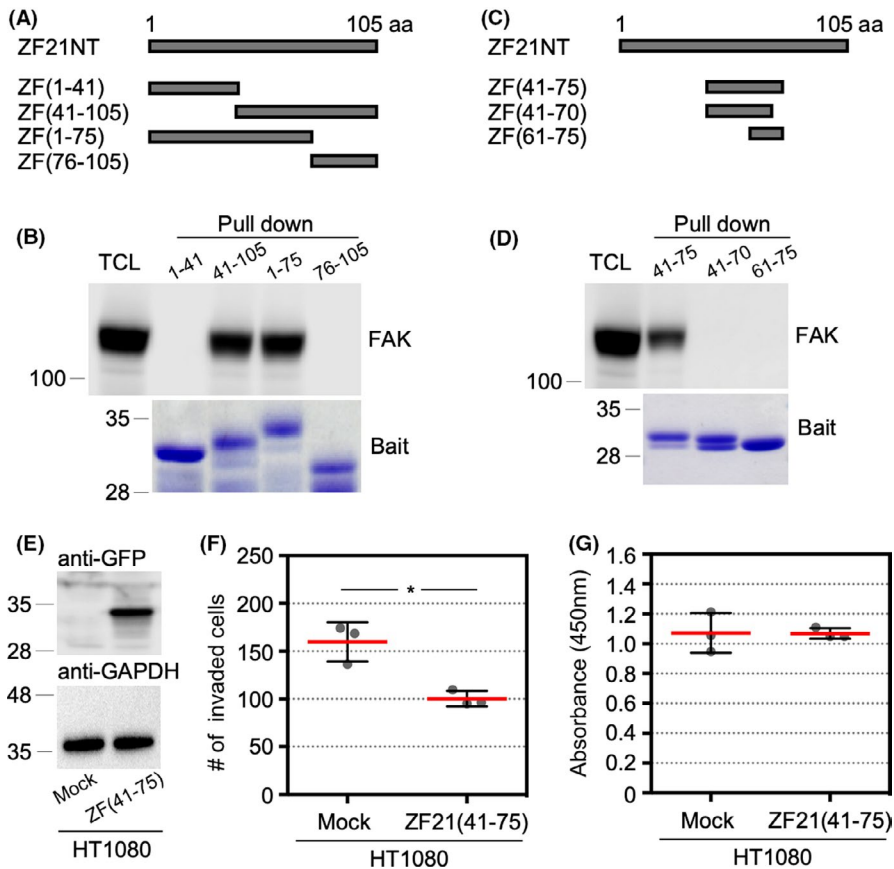


FIGURE 7 Minimizing the ZF21-derived polypeptide having an inhibitory effect on tumor invasion. A, C, Region of ZF21NT-fragmented polypeptide using a bait for the FAK-binding assay. B, D, Pull-down assay of FAK using GST-ZF21 derivatives. (Upper) FAK bound to GST-ZF21 was analyzed by western blotting using the anti-FAK antibody. (Lower) CBB staining of the bait proteins. E, Expression levels of the m1Venus-tagged ZF21(41-75) fragment in HT1080 cells. F, Invasive activity of ZF21(41-75)-expressing cells. G, Cell proliferation activity of ZF21(41-75)-expressing cells. The data show the mean \pm standard error of the mean from 3 independent experiments (F, G). * $P < .05$, unpaired *t* test with Welch correction

functions of FAs and invadopodia. Importantly, we have previously demonstrated that ZF21NT expression showed negligible effects on FAK dephosphorylation and cellular migratory activity in ZF21 knockdown cells,²⁹ suggesting that ZF21NT specifically perturbs ZF21-regulated function. Although ZF21 interacts with multiple regulators of FA turnover, ZF21NT is the only previously identified ZF21-binding partner that binds specifically to FAK. Thus, the interaction of ZF21 with FAK is important for ZF21-dependent tumor invasion.

ZF21 promotes ECM degradation at the invadopodia and the turnover of FAs, resulting in tumor suppression. Our knowledge of the mechanism underlying the dynamics between FAs and invadopodia is still fragmentary. However, recent advances have shed light on the association between invadopodia formation and activity and FA turnover.²³⁻²⁵ FAK has been characterized as a central regulator of FA turnover,³⁸ and has also been reported as having a role in invadopodia formation. Depletion of FAK switches the localization of various phosphotyrosine-containing proteins from FAs to invadopodia, thus upregulating the formation of invadopodia.²⁵ Therefore, FAK inactivation is expected to act as a switch from FA-dependent static adhesion to invadopodia-regulated ECM-degradative adhesion. Interestingly, FAK depletion enhances the formation of ECM-degradative invadopodia, but impairs the invasive activity of the cells.²⁵ This suggests that the balance between the formation of FAs and invadopodia is crucial for the coordination between FA-regulated cellular migration and invadopodia-regulated ECM degradation. ZF21 induces dephosphorylation of FAK through the

elongation of MTs to FAs, implicating ZF21 as a regulator of the spatio-temporal activity of FAK. Our findings suggest a possible role for ZF21 in coordinating the balance between various adhesive structures through its interaction with FAK, which is crucial for tumor invasion and metastasis (Figure 6E). Although the ZF21NT polypeptide effectively inhibited the interaction between ZF21 and FAK, it remains possible that ZF21NT interferes with other, unidentified targets. Further studies are necessary to identify the ZF21-binding sites in FAK. The FAK mutant lacking the ability to bind to ZF21 will greatly help to verify our model.

Some studies have addressed the critical role of FAK in tumorigenesis and tumor acquisition, indicating that tyrosine kinase may be a promising therapeutic target.³⁹ In fact, several types of FAK inhibitors have been developed, and some have been tested in clinical trials for malignant tumors.³⁹⁻⁴¹ Current FAK inhibitors mainly target the kinase domain containing the ATP-binding site to inhibit FAK enzymatic activity. Indeed, several compounds inhibiting FAK kinase activity, such as GSK2256098 and BI 853520, are currently in clinical or preclinical trials.⁴² Unlike these classical FAK inhibitors, ZF21NT affects the function of FAK by inhibiting the turnover of its phosphorylated state at the cellular adhesion sites. Therefore, a combination of the classical FAK inhibitors and ZF21NT could be a promising therapeutic strategy for malignant tumors promoted by FAK. Although ZF21NT, which is composed of 105 aa residues, is too large to use as an inhibitor, we further shortened the FAK-binding region of ZF21 to 35 aa residues at the 41-75 aa region. This fragment polypeptide

ZF21(41-75) inhibited the invasive capacity of the HT1080 cells. However, the ZF21NT polypeptide inhibits tumor invasion more effectively than the ZF21(41-75) polypeptide, demonstrating that the surrounding residues are necessary for the inhibitory effect on tumor invasion.

Future studies focusing on the structural analysis of the FAK/ZF21-derived polypeptide complex will be useful in developing a small inhibitor molecule targeting the interaction between FAK and ZF21. To better understand the ZF21-dependent tumor acquisition mechanism, we intend to utilize the ZF21-derived polypeptides that interact with microtubules, m-Calpain, or SHP-2, in future studies.

ACKNOWLEDGMENTS

We thank Dr. A. Miyawaki for providing the m1Venus cDNA clones and Dr. R. Tsien for providing the mCherry cDNA clones. This work was supported by JSPS KAKENHI (JP 23790109) and the Takeda Science Foundation to MN, JSPS KAKENHI (JP 17K15005) to DH, MEXT KAKENHI (JP 17K09027), the Grant-in-Aid for Scientific Research on Innovative Areas (JP 17H06329) and Research Grant, Princess Takamatsu Cancer Research Fund to NK

DISCLOSURE

The authors have no conflict of interest.

ORCID

Naohiko Koshikawa  <https://orcid.org/0000-0002-4539-888X>

REFERENCES

- Friedl P, Wolf K. Tumour-cell invasion and migration: diversity and escape mechanisms. *Nat Rev Cancer*. 2003;3:362-374.
- Gupta GP, Massague J. Cancer metastasis: building a framework. *Cell*. 2006;127:679-695.
- Steeg PS. Tumor metastasis: mechanistic insights and clinical challenges. *Nat Med*. 2006;12:895-904.
- Wehrle-Haller B, Imhof B. The inner lives of focal adhesions. *Trends Cell Biol*. 2002;12:382-389.
- Zamir E, Geiger B. Molecular complexity and dynamics of cell-matrix adhesions. *J Cell Sci*. 2001;114:3583-3590.
- Petit V, Thiery JP. Focal adhesions: structure and dynamics. *Biol Cell*. 2000;92:477-494.
- Yamaguchi H. Pathological roles of invadopodia in cancer invasion and metastasis. *Eur J Cell Biol*. 2012;91:902-907.
- Eddy RJ, Weidmann MD, Sharma VP, Condeelis JS. Tumor cell invadopodia: invasive protrusions that orchestrate metastasis. *Trends Cell Biol*. 2017;27:595-607.
- Boudreau NJ, Jones PL. Extracellular matrix and integrin signalling: the shape of things to come. *Biochem J*. 1999;339(Pt 3):481-488.
- Liu S, Calderwood DA, Ginsberg MH. Integrin cytoplasmic domain-binding proteins. *J Cell Sci*. 2000;113(Pt 20):3563-3571.
- Critchley DR. Focal adhesions - the cytoskeletal connection. *Curr Opin Cell Biol*. 2000;12:133-139.
- Kechagia JZ, Ivaska J, Roca-Cusachs P. Integrins as biomechanical sensors of the microenvironment. *Nat Rev Mol Cell Biol*. 2019;20:457-473.
- Burridge K, Mangeat P. An interaction between vinculin and talin. *Nature*. 1984;308:744-746.
- Lipfert L, Haimovich B, Schaller MD, Cobb BS, Parsons JT, Brugge JS. Integrin-dependent phosphorylation and activation of the protein tyrosine kinase pp125FAK in platelets. *J Cell Biol*. 1992;119:905-912.
- Ridley AJ, Schwartz MA, Burridge K, et al. Cell migration: integrating signals from front to back. *Science*. 2003;302:1704-1709.
- Sheetz MP, Felsenfeld DP, Galbraith CG. Cell migration: regulation of force on extracellular-matrix-integrin complexes. *Trends Cell Biol*. 1998;8:51-54.
- Albiges-Rizo C, Destaing O, Fourcade B, Planus E, Block MR. Actin machinery and mechanosensitivity in invadopodia, podosomes and focal adhesions. *J Cell Sci*. 2009;122:3037-3049.
- Evans JG, Matsudaira P. Structure and dynamics of macrophage podosomes. *Eur J Cell Biol*. 2006;85:145-149.
- Linder S, Wiesner C, Himmel M. Degrading devices: invadosomes in proteolytic cell invasion. *Annu Rev Cell Dev Biol*. 2011;27:185-211.
- Hoshino D, Koshikawa N, Suzuki T, et al. Establishment and validation of computational model for MT1-MMP dependent ECM degradation and intervention strategies. *PLoS Comput Biol*. 2012;8:e1002479.
- Watanabe A, Hoshino D, Koshikawa N, Seiki M, Suzuki T, Ichikawa K. Critical role of transient activity of MT1-MMP for ECM degradation in invadopodia. *PLoS Comput Biol*. 2013;9:e1003086.
- Gawden-Bone C, Zhou Z, King E, Prescott A, Watts C, Lucocq J. Dendritic cell podosomes are protrusive and invade the extracellular matrix using metalloproteinase MMP-14. *J Cell Sci*. 2010;123:1427-1437.
- Kolli-Bouhafs K, Sick E, Noulet F, Gies JP, De Mey J, Ronde P. FAK competes for Src to promote migration against invasion in melanoma cells. *Cell Death Dis*. 2014;5:e1379.
- Eckert MA, Santiago-Medina M, Lwin TM, Kim J, Courtneidge SA, Yang J. ADAM12 induction by Twist1 promotes tumor invasion and metastasis via regulation of invadopodia and focal adhesions. *J Cell Sci*. 2017;130:2036-2048.
- Chan KT, Cortesio CL, Huttenlocher A. FAK alters invadopodia and focal adhesion composition and dynamics to regulate breast cancer invasion. *J Cell Biol*. 2009;185:357-370.
- Hoshino D, Nagano M, Saitoh A, Koshikawa N, Suzuki T, Seiki M. The phosphoinositide-binding protein ZF21 regulates ECM degradation by invadopodia. *PLoS One*. 2013;8:e50825.
- Nagano M, Hoshino D, Koshikawa N, Akizawa T, Seiki M. Turnover of focal adhesions and cancer cell migration. *Int J Cell Biol*. 2012;2012:310616.
- Nagano M, Hoshino D, Sakamoto T, Akizawa T, Koshikawa N, Seiki M. ZF21 is a new regulator of focal adhesion disassembly and a potential member of the spreading initiation center. *Cell Adh Migr*. 2011;5:23-28.
- Nagano M, Hoshino D, Koshiba S, et al. ZF21 protein, a regulator of the disassembly of focal adhesions and cancer metastasis, contains a novel noncanonical pleckstrin homology domain. *J Biol Chem*. 2011;286:31598-31609.
- Nagano M, Hoshino D, Sakamoto T, Kawasaki N, Koshikawa N, Seiki M. ZF21 protein regulates cell adhesion and motility. *J Biol Chem*. 2010;285:21013-21022.
- Ezratty EJ, Partridge MA, Gundersen GG. Microtubule-induced focal adhesion disassembly is mediated by dynamin and focal adhesion kinase. *Nat Cell Biol*. 2005;7:581-590.
- Glading A, Lauffenburger DA, Wells A. Cutting to the chase: calpain proteases in cell motility. *Trends Cell Biol*. 2002;12:46-54.
- Yu DH, Qu CK, Henegariu O, Lu X, Feng GS. Protein-tyrosine phosphatase Shp-2 regulates cell spreading, migration, and focal adhesion. *J Biol Chem*. 1998;273:21125-21131.
- Stenmark H, Aasland R, Toh BH, D'Arrigo A. Endosomal localization of the autoantigen EEA1 is mediated by a zinc-binding FYVE finger. *J Biol Chem*. 1996;271:24048-24054.

35. Hoshino D, Tomari T, Nagano M, Koshikawa N, Seiki M. A novel protein associated with membrane-type 1 matrix metalloproteinase binds p27(kip1) and regulates RhoA activation, actin remodeling, and matrigel invasion. *J Biol Chem*. 2009;284:27315-27326.
36. Song M, Park JE, Park SG, et al. NSC-87877, inhibitor of SHP-1/2 PTPs, inhibits dual-specificity phosphatase 26 (DUSP26). *Biochem Biophys Res Commun*. 2009;381:491-495.
37. Han S, Mistry A, Chang JS, et al. Structural characterization of proline-rich tyrosine kinase 2 (PYK2) reveals a unique (DFG-out) conformation and enables inhibitor design. *J Biol Chem*. 2009;284:13193-13201.
38. Ilic D, Furuta Y, Kanazawa S, et al. Reduced cell motility and enhanced focal adhesion contact formation in cells from FAK-deficient mice. *Nature*. 1995;377:539-544.
39. Lee BY, Timpson P, Horvath LG, Daly RJ. FAK signaling in human cancer as a target for therapeutics. *Pharmacol Ther*. 2015;146:132-149.
40. Golubovskaya VM, Figel S, Ho BT, et al. A small molecule focal adhesion kinase (FAK) inhibitor, targeting Y397 site: 1-(2-hydroxyethyl) -3, 5, 7-triaza-1-azoniatricyclo [3.3.1.1^{3,7}]decane; bromide effectively inhibits FAK autophosphorylation activity and decreases cancer cell viability, clonogenicity and tumor growth in vivo. *Carcinogenesis*. 2012;33:1004-1013.
41. Cabrita MA, Jones LM, Quizi JL, Sabourin LA, McKay BC, Addison CL. Focal adhesion kinase inhibitors are potent anti-angiogenic agents. *Mol Oncol*. 2011;5:517-526.
42. Mohanty A, Pharaon RR, Nam A, Salgia S, Kulkarni P, Massarelli E. FAK-targeted and combination therapies for the treatment of cancer: an overview of phase I and II clinical trials. *Expert Opin Investig Drugs*. 2020;29:399-409.

How to cite this article: Nagano M, Hoshino D, Toshima J, Seiki M, Koshikawa N. NH₂-terminal fragment of ZF21 protein suppresses tumor invasion via inhibiting the interaction of ZF21 with FAK. *Cancer Sci* 2020;111:4393-4404. <https://doi.org/10.1111/cas.14665>